Journal of Molecular Structure 928 (2009) 158–170

Contents lists available at ScienceDirect

Journal of Molecular Structure

journal homepage: www.elsevier.com/locate/molstruc

Synthesis and spectroscopic studies of charge transfer complexes between chloranilic acid and some heterocyclic amines in ethanol

Amirah S. AL-Attas [a,*], Moustafa M. Habeeb [b], Doaa S. AL-Raimi [a]

[a] Chemistry Department, Girls College of Education, King Abdulaziz University, Jeddah, Saudi Arabia
[b] Chemistry Department, Faculty of Education, Alexandria University, Alexandria, Egypt

ARTICLE INFO

Article history:
Received 2 January 2009
Received in revised form 23 March 2009
Accepted 25 March 2009
Available online 5 April 2009

Keywords:
Spectra
CT-complexes
Amines
Chloranilic acid

ABSTRACT

Charge transfer (CT) complexes formed between 2-amino-4-methoxy-6-methyl-pyrimidine (AMMP), 2-amino-4,6-dimethyl-pyrimidine (ADMP), 3-amino-pyrazole (AP), 3,5-dimethyl-pyrazole (DMP), 3-amino-5-methyl-pyrazole (AMP), 2-amino-4-methyl-thiazole (AMT), 2-amino-5-methyl-1,3,4-thiadiazole (AMTD) and 3-amino-5,6-dimethyl-1,2,4-triazine (ADMT) as electron donors with the π-acceptor chloranilic acid (CHA) were investigated spectrophotometrically in ethanol. Minimum–maximum absorbances method has been used for estimating the formation constants of the charge transfer reactions (K_{CT}). It has been found that K_{CT} depends on the pKa of the studied donors. Job's method of continuous variation and photometric titration studies were used to detect the stoichiometric ratios of the formed complexes and they showed that 1:1 complexes were produced. The molar extinction coefficient (ε), oscillator strength (f), dipole moment (μ), charge transfer energy (E_{CT}), ionization potential (I_P) and the dissociation energy (W) of the formed complexes were estimated, they reached acceptable values suggesting the stability of the formed CT-complexes. The solid CT-complexes were synthesized and characterized by elemental analyses, ^{1}HNMR and FTIR spectroscopies where the formed complexes included proton and electron transfer.

1. Introduction

In through last few decades, charge transfer complexes play an essential role in the analysis of some drugs in pure form or pharmaceutical preparation [1,2], solar energy storage [3] and surface chemistry [4] as well as many biological fields [5], charge transfer complexes are found to take part in many chemical reactions, like addition, substitution and condensation [6–8]. These complexes have great attention for non-linear optical materials and electrical conductivities [9–12]. For their wide applications, extensive studies on CT-complexes of π acceptors have been performed. Pyrimidines, thiazoles, pyrazoles and triazines are very important heterocyclic compounds. They considered to be important not only because they are on integral part of genetic materials viz., DNA and RNA as nucleotides and nucleosides also they have important numerous biodynamic properties and biological activities such as bactericides, fungicides, vermicides and medicines [13–19]. Charge transfer complexes of organic species are intensively studied because of their special type of interaction, which is accompanied by transfer of an electron from the donor to the acceptor [20,21]. Also protonation of the donor from acidic acceptors are generally a route for the formation of ion pair adducts [22–24].

In connection with the study of CT-complexes and due to the biological importance and industrial applications of the amino heterocyclic donors, the present article included a continuation on the CT complexes through studying and characterization of charge transfer complexes of some amines of (pyrimidines, thiazoles, pyrazoles and triazines) as electron donors (Scheme 1) with chloranilic acid as π-electron acceptor in ethanol. Formations constants (K_{CT}), molar extinction coefficient (ε), oscillator strength (f), dipole moment (μ), energy (E_{CT}), ionization potential (I_P) and dissociation energy (W) of the formed CT-complexes were estimated and evaluated. The synthesis and characterization of the solid CT-complexes are important aims of this work.

2. Experimental

2.1. Materials

All chemicals used were of analytical grade. Chloranilic acid (98%) (CHA), ethanol absolute PA (99.5%) were obtained from (BDH). 2-Amino-4-methoxy-6-methyl-pyrimidine (99%) (AMMP), 2-amino-4,6-dimethyl-pyrimidine (98%) (ADMP), 3-aminopyrazole (98%) (AP), 3,5-dimethyl-pyrazole (98.5%) (DMP), 3-amino-5-

* Corresponding author. Tel.: +966 505677583; fax: +966 266732234.
E-mail address: amirh-alattas@hotmail.com (A.S. AL-Attas).

0022-2860/$ - see front matter © 2009 Elsevier B.V. All rights reserved.
doi:10.1016/j.molstruc.2009.03.025

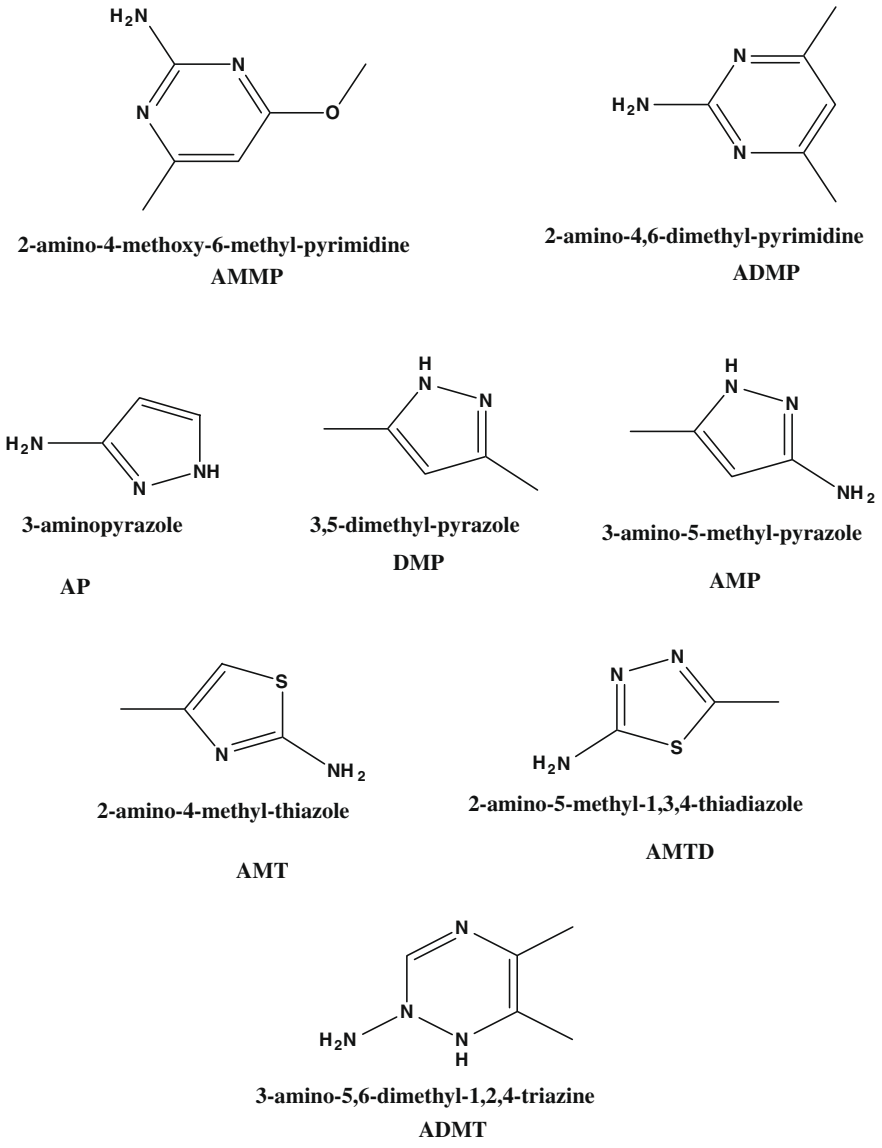

Scheme 1. Chemical Structures of donors.

methyl pyrazole (97%) (AMP), 2-amino-4-methyl-thiazole (98%) (AMT), 2-amino-5-methyl-1,3,4-thiadiazole (97%) (AMTD) and 3-amino-5,6-dimethyl-1,2,4-triazine (98%) (ADMT) were purchased from Acros organic. The heterocyclic donor amines and chloranilic acid were used without further purification.

2.2. Preparation of standard solutions of the donors and acceptor

Stock solutions of the donors (10^{-2} M) and CHA (5×10^{-3} M) were freshly prepared before each series of measurements by dissolving precisely weighed amounts in the appropriate volume of the solvent. The stock solutions of donors and acceptor were protected from light. Solutions for spectroscopic measurements were made by mixing appropriate volumes of stock donors and CHA solutions and pure solvent.

2.3. Instrumentation and physical measurements

2.3.1. Electronic absorption spectra

The electronic absorption spectra were recorded in the region 700–250 nm using UV–vis model Shimadzu UV-1601 with personal spectroscopy software version 3.7, connected to Shimadzu TCC-ZUOA temperature controller.

2.3.2. Infrared spectra

The infrared spectra of the prepared solid CT-complexes were measured as KBr discs on Shimadzu FTIR-8400 S Fourier transform infrared spectrophotometer (Japan).

2.3.3. ^{1}HNMR spectra

^{1}HNMR spectra were obtained on Bruker 600 MH_Z using TMS as an internal reference and d_6-DMSO as the solvent.

2.3.4. Elemental analyses

C, H and N contents were determined with the Micro Analyser, Perkin Elmer 2400 (USA).

2.3.5. Potentiometric titration

pH-metric titrations were performed using a Metrohm 744 pH meter (Metrohm, Herisau, Switzerland). The combined glass electrode was standardized using buffer solutions from Metrohm. All titrations were carried out at room temperature.

2.4. Preparation of solid CT-complexes

The solid CT-complexes between the donors and the acceptor were prepared by mixing equimolar amounts of donor and acceptor in acetonitrile. The resulting color complex solutions were allowed to evaporate slowly at room temperature where the solid precipitated after reduction of the volume of the solvent. The separated complexes were filtered off, washed several times with acetonitrile, and then collected and dried; the analytical data of the CT-complexes (C, H, N Content) along with some of the physical properties are listed in Table 1.

2.5. Photometric titration

Photometric titrations at 528–530 nm for the reaction between the studied donors and CHA in ethanol solvent were carried out as follows; the concentration of CHA was kept constant at 5×10^{-4} M, whereas that of the donors were changed over the wide range from 5×10^{-5} to 2×10^{-3} M. The donor–acceptor molar ratio (C_D:C_A) obtained in this case varied from 0.25 to 4. The peak absorbances appear in the spectra that were assigned to the formed CT-complexes were measured and plotted as a function of the ratio (C_D:C_A) according to the known method [25].

Table 1
Elemental analysis, stoichiometry, melting point, color of the CT-complexes of CHA with the donors.

Donor	Expected			Found			Stoichiometry	mp °C	Colour
	C	H	N	C	H	N			
AMTD	33.32	2.16	12.96	33.35	2.11	12.29	1:1	208.3	Brown
ADMT	39.62	3.00	16.81	40.23	2.91	17.62	1:1	185.0	Brown
DMP	43.26	3.28	9.18	43.34	3.08	9.06	1:1	210.0	Purple
AP	36.98	2.40	14.83	37.54	2.92	15.04	1:1	205.0	Brown
AMP	39.20	2.94	13.72	39.52	2.38	13.80	1:1	186.0	Brown
AM	37.13	2.48	8.66	37.60	2.33	8.91	1:1	209.0	Purple
AMMP	41.38	3.16	12.07	41.42	2.87	12.14	1:1	216.8	Purple
ADMP	43.37	3.31	12.65	43.58	2.18	12.84	1:1	205.7	Brown

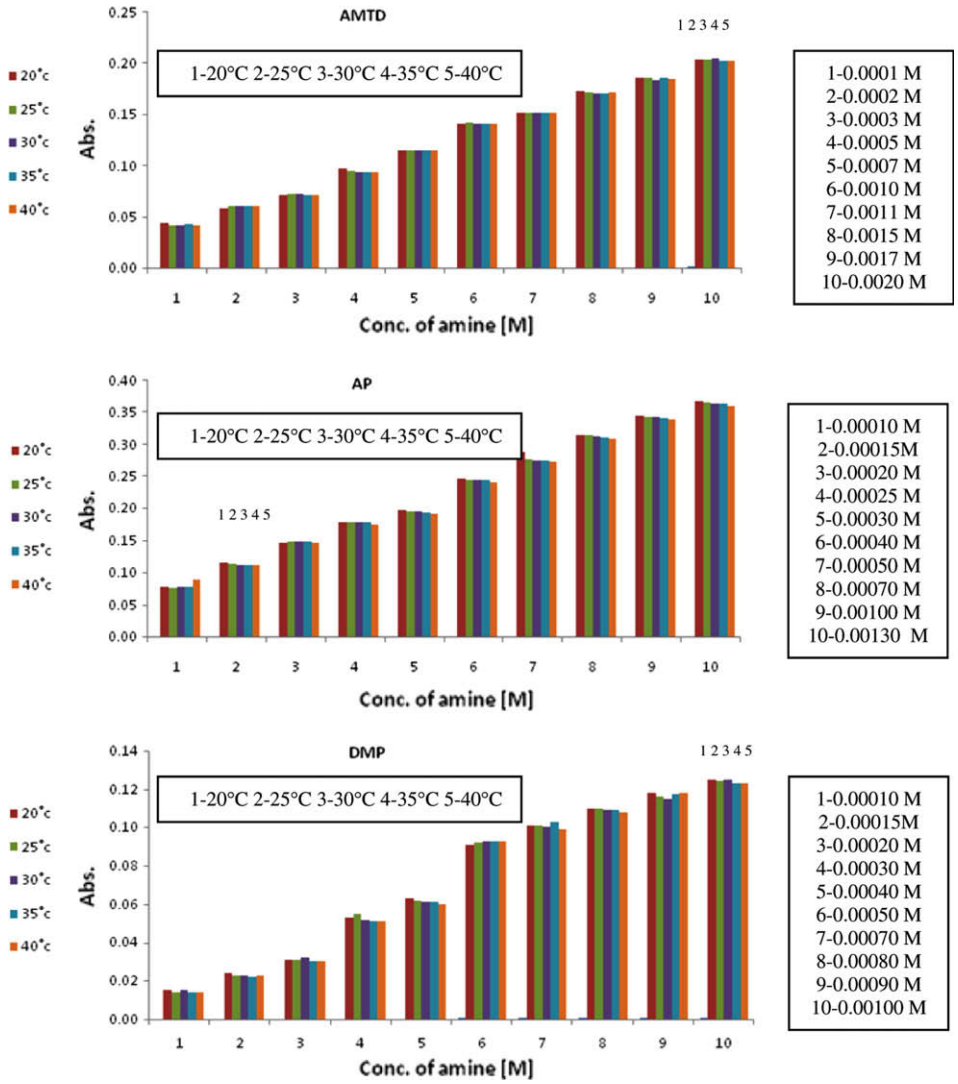

Fig. 1. Effect of donor concentrations on the absorbance of CT-complexes with 5×10^{-4} M CHA at different temperatures in ethanol.

2.6. Determination of pKa for donors

Twenty-five milliliter of 1×10^{-2} M from each of the donor (B) solutions were transferred to the titration cell and titrated with 5×10^{-1} M HCl solution in presence of stream of dry nitrogen gas. The pH value was recorded after through stirring following each addition (0.05 ml) at room temperature. The pKa is estimated from the following equation [26].

$$pKa = pH + \log[BH^+]/[B]$$

2.7. Determination of the formation constants of the CT-complexes (K_{CT})

For the purpose of UV–vis spectral determination of the formation constants (K_{CT}), we applied the minimum–maximum absorbances method according to the following procedure. One

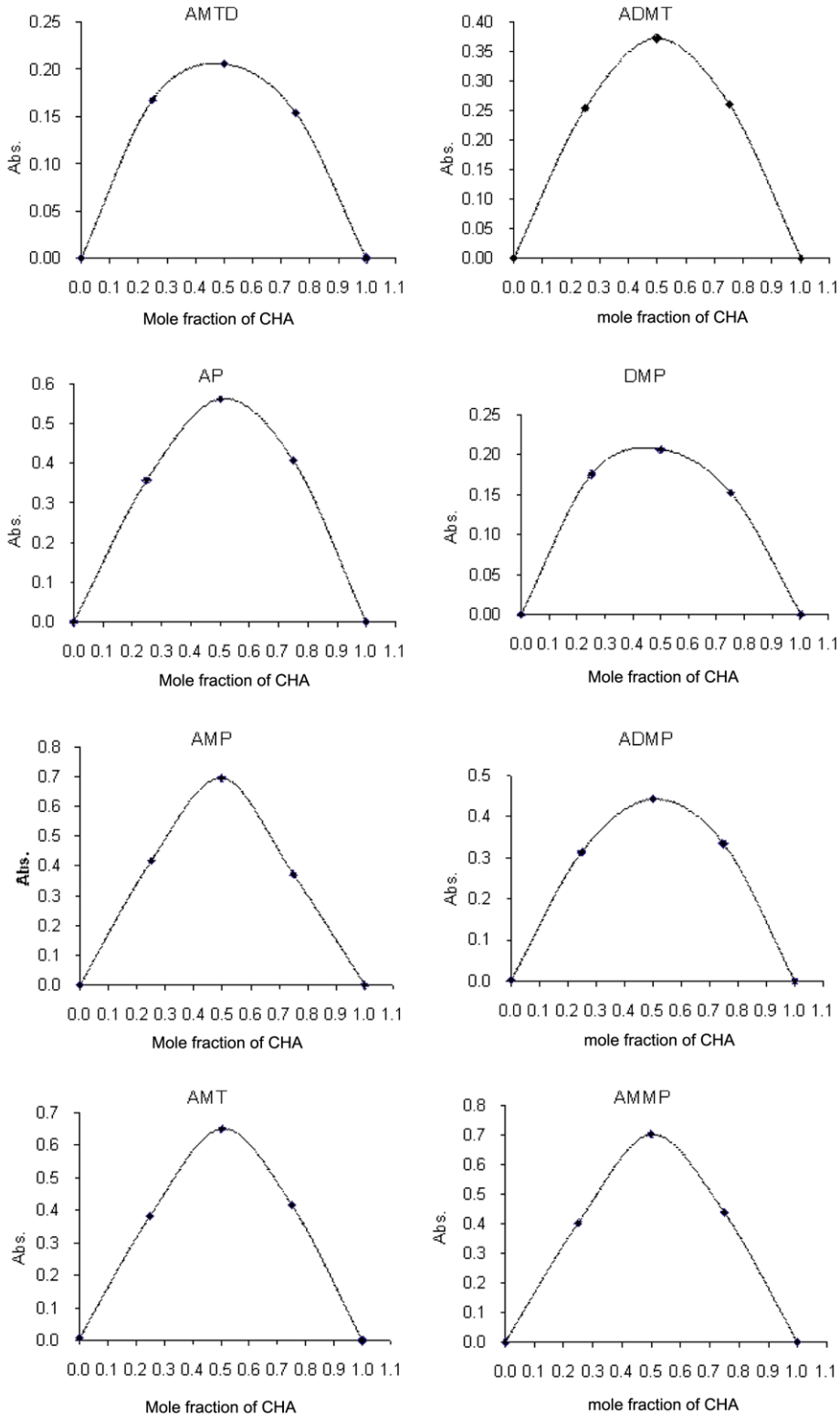

Fig. 2. Jobs plot of CT-complexes of CHA with donors in ethanol.

milliliter (CTA) of freshly prepared stock solution (5×10^{-3} M) was transferred into a series of 10 ml calibrated flasks. To each of these were added different concentrations of the freshly stock donor solution (1×10^{-2} M) and diluted to the mark with ethanol. The least concentration of the added amine led to the minimum absorbance of the complex (A_{min}). The concentration of the donor is increased gradually and the absorbance is recorded at the absorption band of the CT-complexes (A_{mix}) until we got the highest constant absorbance (A_{max}). The CT-formation constants (K_{CT}) were estimated as given by the following equation:

$$A_{max} = A_{mix} + \frac{A_{mix} - A_{min}}{K_{CT} \times C_{amine}} \quad (1)$$

where A_{max}: Maximum absorbance of the complex. A_{min}: Minimum absorbance of the complex. A_{mix}: Complexes absorbance values between A_{max} and A_{min}. C_{amine}: Concentration of the added amine in mol L^{-1}.

The set of equilibrium constants were averaged [27].

3. Results and discussion

3.1. Effect of CHA concentration

The effect of reagent concentration was studied by following the absorbance of the CT-complexes between varied amounts of 5×10^{-3} M CHA with 1 ml of 2×10^{-3} M from each of the donors in 10 mL calibrated flasks and diluted to the mark with ethanol. It has been found that maximum constant absorbances of the CT-complexes were obtained with 1 mL of 5×10^{-3} M CHA.

3.2. Effect of reaction time and temperature

Reaction time and temperature was determined by following the absorbance of the formed purple color of CT-complex development upon mixing 1 mL of 5×10^{-3} M CHA solution with various concentrations from each of the donors in 10 mL calibrated flasks and diluted to the mark with ethanol. It has been found that the purple color is formed instantly at room temperature and the CT-complexes were stable within 2 h.

The effect of temperature on the formed complexes was studied, where the formed complexes were stable up to 40 °C as shown in Fig. 1.

3.3. Stoichiometric ratios of the formed CT-complexes

The composition of the formed CT-complexes were determined by applying Job's method of continuous variations [28] and photometric titrations. Fig. 2 represents the continuous variation method curves according to Job's Method, the maximum absorbance was recorded at 0.5 mol fraction indicating 1:1 CT-complex formation (donor:acceptor). Fig. 3 represents the photometric titrations where two straight lines were produced intercepting at 1:1 ratio (donor:acceptor).

3.4. Spectral characteristics of the CT-complexes

The electronic absorption spectra of the CT-complexes between the donors and acceptor were carried out in ethanol solvent, illustrative examples of the electronic spectra are shown in Fig. 4. once the donor and acceptor solutions are mixed, strong change in color was observed and associated with the appearance of a new symmetrical long wave length absorption band attributing to the π–π^* transition of the formed CT-complexes. These bands were located at 530 nm for the complexes [(AMMT) (CHA)], [(ADMP) (CHA)], [(AP) (CHA)] and [(ADMT) (CHA)], at 529 nm for the complexes [(AMTD) (CHA)], [(AMP) (CHA)] and [(AMT) (CHA)] and at 528 nm for the complex [(DMP) (CHA)], respectively.

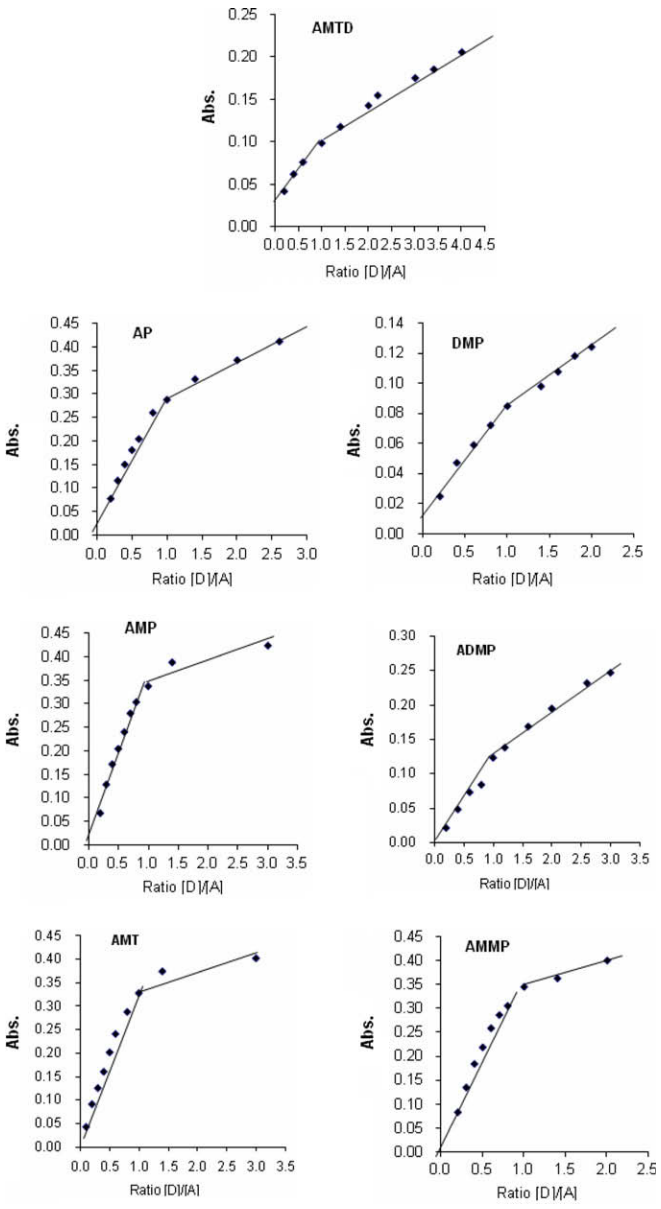

Fig. 3. Molar ratio plots for CT-complexes of CHA with donors in ethanol.

The electronic spectra were scanned against the same electron acceptor concentration as in the working solution to eliminate the possible overlap that may arise between CT-complex band and that of the acceptor.

3.5. Mechanism of the CT reaction

The new, low energy absorptions observed in ethanol solutions containing both a donor and acceptor have been described by Mulliken [29] as charge CT transitions involving the excitation of an electron on the donor to an empty orbital on the acceptor. As indicated in Scheme 2, the origin of the bands of EDA complex is understood to result from promotion of an electron from filled π-donor orbital to the LUMO of CHA producing a

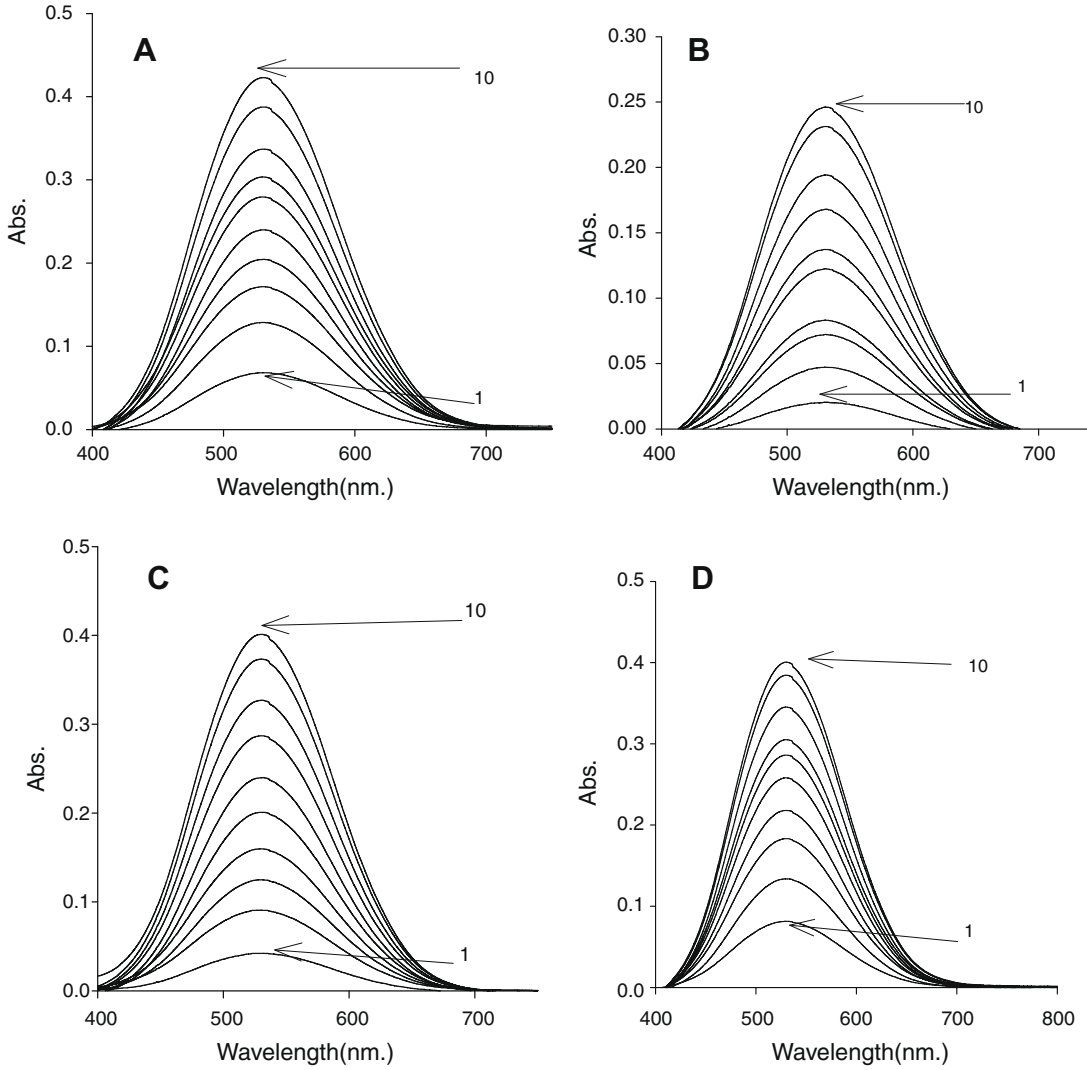

Fig. 4. Electronic spectra of the CT-complexes formation between [5×10^{-4} M] CHA in ethanol in presence of various concentrations of (A) AMP (1) 1×10^{-4} – (10) 1.5×10^{-3} M, (B) ADMP (1) 1×10^{-4} – (10) 1.5×10^{-3} M, (C) DMP (1) 1×10^{-4} – (10) 1×10^{-3} M and (D) AMMP (1) 1×10^{-4} – (10) 1×10^{-3} M.

pair of radical ions. Hence one concludes that the observed new low energy absorption bands are presumably attributed to the radical anion of chloranilic acid (Scheme 3).The energy associated with each transition will depend on the relative energies of the initial and electronic state [30].

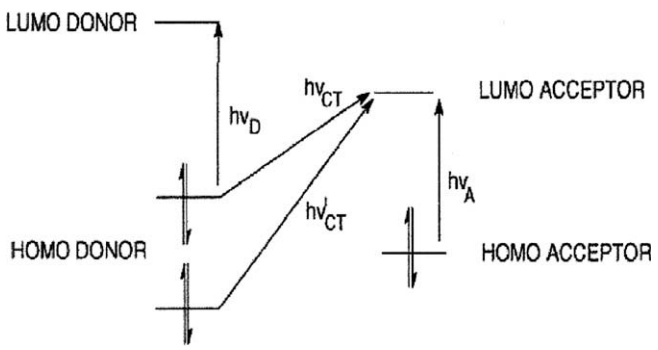

Scheme 2. Charge-transfer transition from HOMOs of the donor compounds and LUMOs of the acceptor compounds.

3.6. Formation constants of the charge transfer reaction (K_{CT})

Based on the electronic spectra of the formed complexes at various concentrations of the donors, K_{CT} were estimated by using the minimum–maximum absorbances method, the results are collected in Tables 2 and 3. Generally, K_{CT} recorded higher values suggesting the formation of stable CT-complexes. It has been found that K_{CT} of the formed CT-complexes depend on the pKa values of the electron donors where a direct proportionality between K_{CT} and pKa values was found except for the CHA–ADMP complex (Fig. 5). It seems that the symmetry of ADMP donor led to the formation of a bifurcated hydrogen bonding interaction between the carbonyl and hydroxyl groups of chloranilic acid with the amino group and the ring nitrogen of ADMP. This hydrogen bonding reduces the electron density of the π-system of ADMP leading to a lower K_{CT} value [31]. This situation will be further confirmed by FTIR measurements in Section 3.9. The higher value of K_{CT} for CHA–AMMP charge transfer complex is certainly attributed to the presence of the strongly electron donating methoxy group and the absence of the bifurcated hydrogen bonding beside the higher pKa value of AMMP.

The oscillator strength (f) which is a dimensionless quantity used to express the transition probability of the CT band [32]

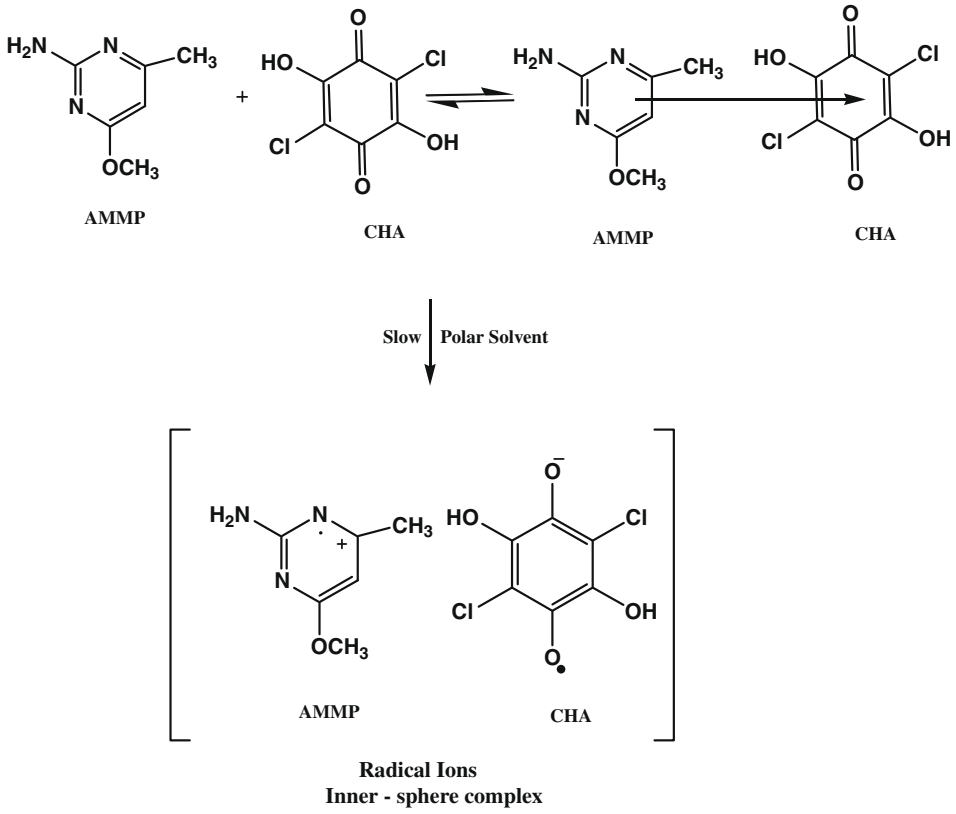

Scheme 3. The molecular structure of compound and charge-transfer transition between CHA and donors.

and the transition dipole moment (μ) of the CT-complexes [33]. The following expressions [34] are commonly used to calculate these two and the results are compiled in Table 4.

$$f = 4.32 \times 10^{-9}[\varepsilon_{max}\ \Delta\nu_{1/2}], \quad (2)$$

$$\mu = 0.0958[\varepsilon_{max}\ \Delta\nu_{1/2}/\nu_{max}]^{1/2} \quad (3)$$

where $\Delta\nu_{1/2}$ is the half band width at half absorbance, ε_{max} and ν_{max} are the extinction coefficient and wave number at the maximum absorption peak of the CT-complex, respectively. As clearly observed from Table 4, the donors with higher pKa values recorded higher oscillator strengths (f) and higher dipole moments (μ) which could be attributed to the higher concentration of the produced chloranilic acid radical anion. The complex CHA–ADMP reached small values of both (f) and (μ) in concordant with its lower K_{CT} value. The small values of both (f) and (μ) for the lower pKa donors confirmed the formation of a lower concentration of chloranilic acid radical anion.

Table 2
Minimum, maximum and mixture concentrations (M) of the added donors at 25 °C.

Donor	$C_{min} \times 10^{-4}$	$C_{max} \times 10^{-4}$	$C_{mix} \times 10^{-4}$							
AMTD	1.00	20	2.00	3.00	5.00	7.00	10.00	11.00	15	17
ADMT	1.00	15	2.00	3.00	4.00	5.00	6.00	8.00	10	13
DMP	1.00	10	1.50	2.00	3.00	4.00	5.00	7.00	8	9
AP	1.00	13	1.50	2.00	2.50	3.00	4.00	5.00	7	10
AMP	1.00	15	1.50	2.00	2.50	3.00	3.50	4.00	5	7
ADMP	1.00	15	2.00	3.00	4.00	5.00	6.00	8.00	10	13
AMT	0.50	7	1.00	1.50	2.00	2.50	3.00	3.50	4	5
AMMP	1.00	10	1.50	2.00	2.50	3.00	3.50	4.00	5	7

Table 3
Minimum–maximum absorbance's data and CT-formation constants at 25 °C.

Donor	pKa	A_{min}	A_{max}	A_{mix}								K_{CT} (L mol^{-1}) $\times_{10}{}^{3}$
AMTD λ_{max} = 529 nm	3.56	0.042	0.204	0.061	0.073	0.095	0.116	0.143	0.152	0.172	0.186	1.83
ADMT λ_{max} = 530 nm	3.94	0.055	0.308	0.101	0.123	0.150	0.156	0.190	0.219	0.246	0.262	1.99
DMP λ_{max} = 528 nm	4.28	0.014	0.124	0.023	0.031	0.055	0.062	0.092	0.101	0.110	0.116	4.14
AP λ_{max} = 530 nm	4.30	0.078	0.366	0.115	0.149	0.180	0.197	0.245	0.278	0.315	0.343	4.17
AMP λ_{max} = 529 nm	4.64	0.079	0.418	0.126	0.169	0.200	0.238	0.282	0.302	0.335	0.384	4.51
ADMP λ_{max} = 530 nm	5.11	0.023	0.251	0.023	0.049	0.074	0.085	0.125	0.141	0.172	0.197	2.63
AMT λ_{max} = 529 nm	5.62	0.051	0.408	0.051	0.085	0.130	0.176	0.215	0.264	0.298	0.325	4.65
AMMP λ_{max} = 529 nm	5.71	0.089	0.401	0.122	0.165	0.212	0.236	0.276	0.304	0.342	0.370	4.91

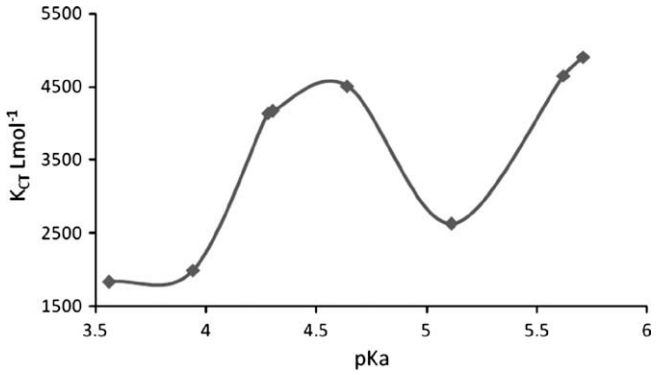

Fig. 5. Correlation between K_{CT} and pKa of donors.

The standard free energy changes of complexation (ΔG°) were also calculated from the formation constant (K_{CT}) using the following equation [35].

$$\Delta G^{\circ} = -2.303\,RT\ \log\ K_{CT} \quad (4)$$

The dissociation energy (W), can be calculated from the corresponding CT energy E_{CT}, ionization potential of the donor (I_P) and electron affinity of the acceptor (E_A) using the relationship [36]:

$$E_{CT} = I_P - E_A - W \quad (5)$$

The energy of the π–π^* interaction (E_{CT}) is calculated using the following equation [37a]:

$$E_{CT} = 1243.667/\lambda_{CT}\ \text{nm} \quad (6)$$

where λ_{CT} is the wavelength of the CT band of the complexes. The E_{CT} values calculated from Eq. (6) are listed in Table 4.

The ionization potential values of the donors are calculated by using the Eq. (7):

$$I_P = a + b(h\nu_{max}) \quad (7)$$

where $h\nu_{max}$ is the π–π^* transition energy in electron volts eV, a and b are 5.11 and 0.701 [38], 4.39 and 0.857 [39] or 5.156 and 0.778 [40], respectively. The mean value calculated by these methods and the values of (W) are collected in Table 4.The electron affinity (E_A) of CHA is 1.1 eV [37b].

Returning to Table 4 one observes that the ionization potential of the donors are constant confirming that the same molecular orbital of the donors π overlaps with the same π^* of the acceptors. On the other hand, the constancy of the ionization potential indicated that I_p has a limited effect on the stability of the formed complexes. The calculated values of the dissociation energy (W) of the charge transfer excited states of the studied complexes are constant suggesting that the investigated complexes are reasonably

Table 4
Energy, ionization potential, dissociation energy, oscillator strength, dipole moment and free energy of CT-complex formation in ethanol.

Donor	pK_a	E_{CT} (eV)	I_P (eV)	W (eV)	ΔG° (k J mol^{-1})	$f \times 100$	μ (Debye)
AMTD	3.56	2.35	6.72	3.27	4.48	6	2.67
ADMT	3.94	2.35	6.72	3.27	4.53	1	3.43
DMP	4.28	2.36	6.76	3.26	5.05	8	2.93
AP	4.30	2.35	6.72	3.27	4.97	2	4.69
AMP	4.64	2.35	6.72	3.27	5.02	17	4.43
ADMP	5.11	2.35	6.72	3.27	4.69	10	3.38
AMT	5.62	2.35	6.72	3.27	5.93	17	4.31
AMMP	5.71	2.35	6.72	3.27	5.07	25	5.27

Table 5
Quantitative parameters of the formed CT-complexes in ethanol.

Parameters	AMTD λ_{max} = 529 nm	ADMT λ_{max} = 530 nm	DMP λ_{max} = 528 nm	AP λ_{max} = 530 nm	ADMP λ_{max} = 530 nm	AMT λ_{max} = 529 nm	AMMP λ_{max} = 529 nm	AMP λ_{max} = 529 nm
Beer's law limits (μg ml^{-1})	23–126	12–74	9–48	8–33	12–73	5–34	20–55	9–33
Limit of detection (μg ml^{-1})	19.11	5.76	7.26	3.79	10.29	2.80	5.09	1.44
Limit of quantification (μg ml^{-1})	63.33	19.04	24.37	12.64	34.21	9.39	16.98	9.28
Molar absorptivity, (ε) (L mol^{-1} cm^{-1})	100.05	256.86	151.79	564.57	236.86	1125.1	708	820.57
Regression equation[a]	$y = 0.0009x + 0.0423$	$y = 0.0021x + 0.0486$	$y = 0.0016x + 0.0124$	$y = 0.0068x + 0.0281$	$y = 0.0019x - 0.0007$	$y = 0.0099x + 0.0486$	$y = 0.0051x + 0.0268$	$y = 0.0084x - 0.0043$
Intercept (a)	0.0423	0.0486	0.0124	0.0281	−0.0007	0.0486	0.0268	−0.0043
Slope (b)	0.0009	0.0021	0.0016	0.0068	0.0019	0.0099	0.0051	0.0084
Confidence interval of intercept (α)	0.0423 ± 0.0052	0.0486 ± 0.0037	0.0124 ± 0.0035	0.0281 ± 0.0092	0.0007 ± 0.0061	0.0486 ± 0.0087	0.0268 ± 0.0119	−0.0043 ± 0.0089
Confidence interval of slope (β)	0.0009 ± 0.0001	0.0021 ± 0.0001	0.0016 ± 0.0001	0.0068 ± 0.0004	0.0019 ± 0.0001	0.0099 ± 0.0004	0.0051 ± 0.0003	0.0084 ± 0.0004
Correlation coefficient (r)	0.9942	0.9955	0.9811	0.9843	0.9837	0.9643	0.9876	0.9920

[a] $A = a + bC$, where A is the absorbance and C is the concentration in μg ml^{-1}.

Table 6
Precision and accuracy of the formed CT-complexes in ethanol.

Donor	Amount taken (μg ml^{-1})	Amount found (μg ml^{-1})	Rec. (%)	$\overline{X}$	SD	RSD	$\lvert\overline{X}-\mu\rvert$	$\frac{\pm t_{n-1}S}{\sqrt{n}}$	Confidence limits
AMMP	25.05	25.73	102.72	100.23	2.26	2.26	0.23	±3.60	100.23 ± 3.60
	32.01	32.39	101.19						
	41.75	41.61	99.56						
	45.92	44.75	97.45						
AP	10.80	10.72	99.26	103.07	3.32	3.22	3.07	±8.25	103.07 ± 8.25
	18.28	18.96	105.31						
	29.08	30.43	104.64						
ADMT	31.04	30.67	98.81	99.160	0.33	0.33	0.84	±0.82	99.16 ± 0.82
	55.86	55.43	99.23						
	65.79	65.43	99.45						
DMP	24.03	24.13	100.42	101.11	0.51	0.50	1.11	±0.81	101.11 ± 0.81
	33.65	34.13	101.43						
	40.38	41.00	101.54						
	46.14	46.63	101.06						
AMTD	46.06	45.22	98.18	99.620	1.34	1.35	0.38	±3.33	99.62 ± 3.33
	56.42	56.33	99.84						
	69.09	69.66	100.83						
AMP	17.48	17.30	98.97	99.910	1.17	1.17	0.09	±2.91	99.91 ± 2.91
	27.19	27.77	99.53						
	31.08	31.46	101.22						

t = 3.182 for n = 4 at 95% confidence level.
t = 4.303 for n = 3 at 95% confidence level.
SD, standard deviation.
RSD, relative standard deviation.

strong and stable under the studies conditions with higher resonance stabilization energy [41].

As clearly observed in Table 4 the negative values of the free energy (ΔG°) suggested the simultaneous production of the CT-complexes. This is also supported by the small values of the CT energy (2.3 eV).

3.7. Quantification parameters

The quantification parameters of the formed CT-complexes are compiled in Tables 5 and 6 where good ranges of different donors concentration obeyed Beer's law were found under the optimum conditions. The limit of detection and limit of quantification recorded small values confirming the validity of the method for donors determination. On the other hand, the regression equation predicted small values of slope, intercept and good correlation coefficient (r) near 0.99 suggesting a very good linear relationship.

3.8. Precision and accuracy of the method

The accuracy of the method was established by performing three and four analyses on solution containing three and four different amounts within the Beer's law limits of each donor. The % recovery recorded values near 100% confirming the accuracy of the method. Moreover the standard deviation recorded small values suggesting the higher precision of the method. Comparison of (the difference between the determined value and the true value) with the indeterminate error $\frac{\pm t_{n-1}S}{\sqrt{n}}$ was carried out and the results were compiled in Table 6 [42]. It was found that ($X^{-}-\mu$) are less than $\pm tS/\sqrt{n}$ indicating that no significant difference between the mean and the true values.

3.9. Characterization of the solid CT-complexes

3.9.1. Elemental analyses

The chemical analysis (Table 1) data of the isolated color solid CT-complexes indicated the formation of 1:1 CT-complexes. The formed CT-complexes are predominantly of π–π^{*} type based on the planarity of the donors molecules [43].

3.9.2. FTIR spectra

The formation of CT-complexes during the reaction of the donors with chloranilic acid is strongly supported by observing the main infrared bands of the donor and acceptor in the product spectra. However, the bands of the donor and acceptors in the complexes spectra reveal small shifts in intensities compared with those of the free donors and acceptor. This should be attributed to the expected symmetry and electronic structure change upon the formation of CT-complexes.

Chloranilic acid is a strong electron acceptor to form stable CT-complexes with the donors. Beside this function CHA is a strong acid (pK_1 = 1.07 and pK_2 = 2.24) [44], hence a proton transfer from CHA to the donors is expected.

Comparison of the infrared spectral bands of the free donors and acceptor with the corresponding ones appearing in the IR spectra of the CT-complexes (Figs. 6 and 7) revealed the following:

1. The carbonyl C=O stretching vibration appearing at 1662 cm^{-1} in the IR spectrum of (CHA) is shifted to 1643, 1637, 1620 1635,1629 and 1620 cm^{-1} in the FTIR spectra of the CT-complexes of CHA with AP,AMT,ADMT, DMP AMTD and AMP, respectively.
2. The ν_{C-C1} vibrations appearing at (854, 839, 752 cm^{-1}) in the IR spectrum of CHA are shifted to (840, 769, 719 cm^{-1}), (839, 761, 717 cm^{-1}), (840, 827, 781 cm^{-1}), (790, 779, 721 cm^{-1}), (839, 752, 705 cm^{-1}) and (783, 759, 644 cm^{-1}) in the FTIR spectra of the CT-complexes of CHA with AP, AMT, ADMT, DMP, AMTD and AMP, respectively.
3. The asymmetric and symmetric stretching vibrations of the amino group ν^{as} (NH_2), ν^{s} (NH_2) appearing at (3439, 3300 cm^{-1}) and (3255, 3091 cm^{-1}) in the IR spectra of the donors (AMT, AMTD) are not affected on complexation with CHA suggesting that they are not participating in hydrogen

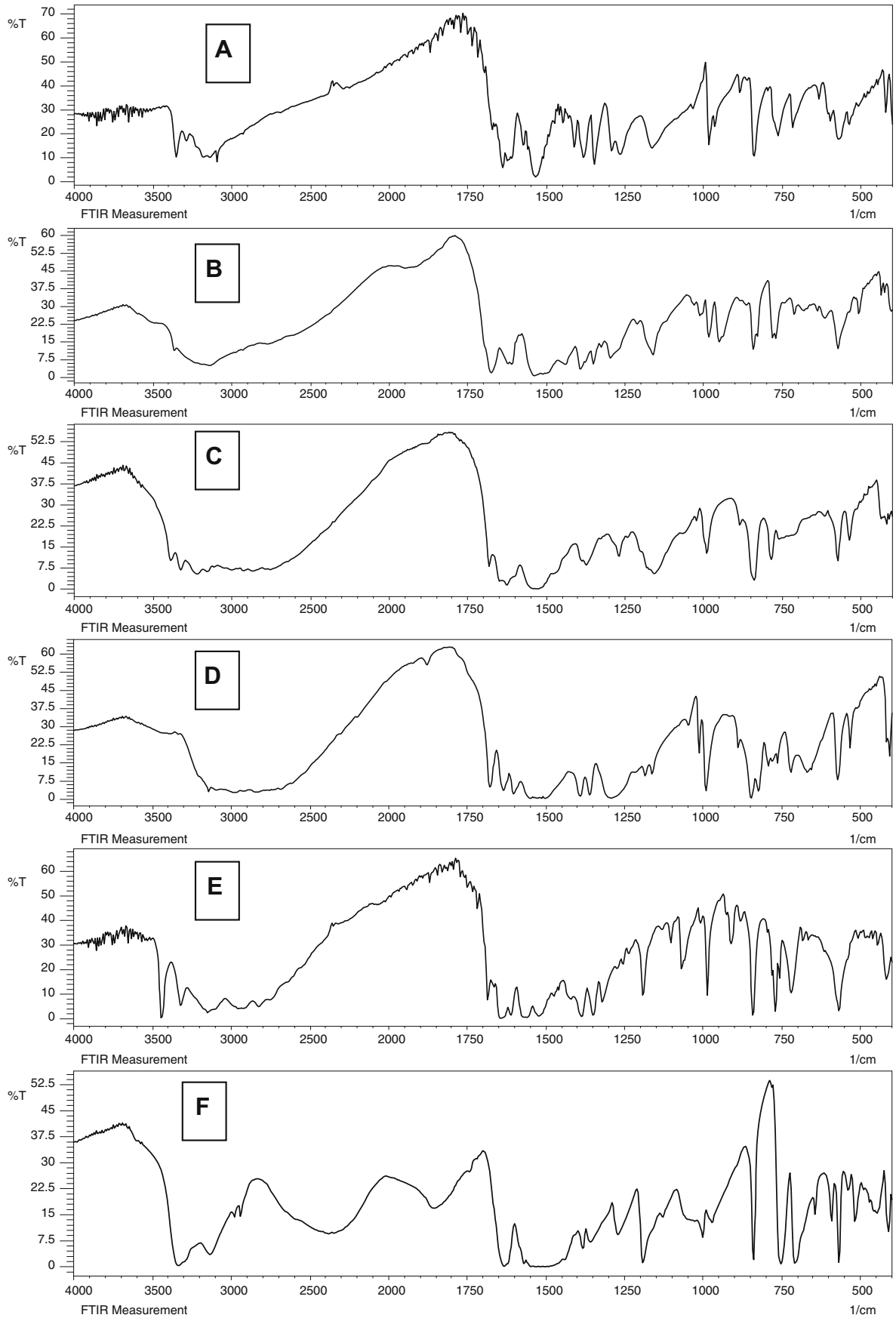

Fig. 6. FTIR spectra of CT-complexes of CHA and donors [(A) AMT, (B) ADMT, (C) AMP, (D) DMP, (E) AP, (F) AMTD] in the range 4000–400 cm^{-1}.

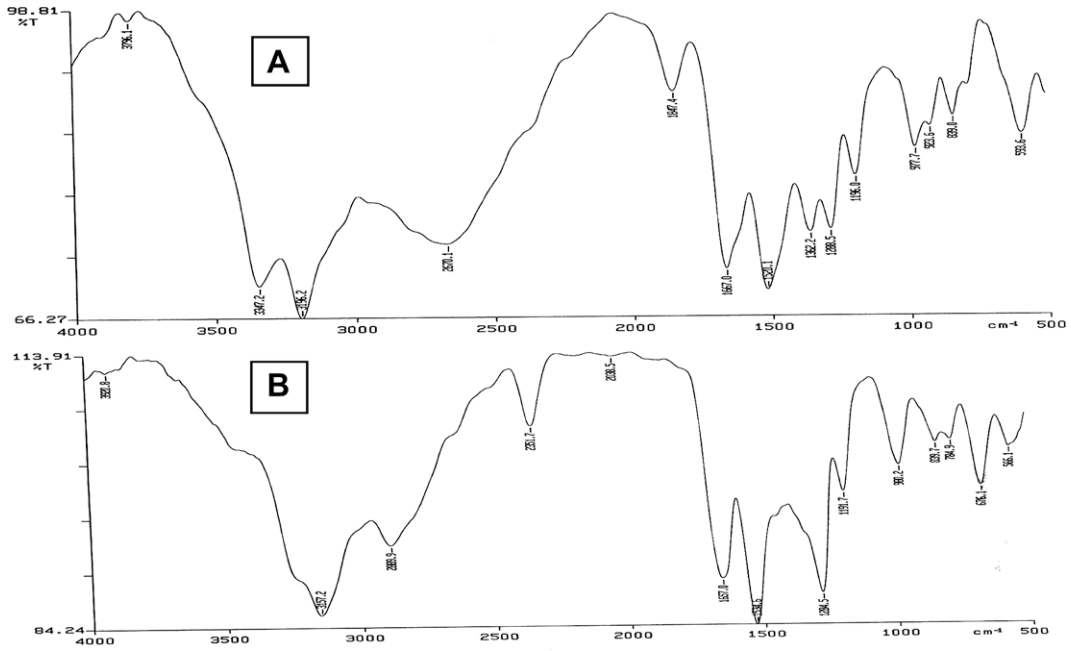

Fig. 7. FTIR spectra of CHA and donors [(A) AMMP and (B) ADMP] in the range 4000–400 cm^{-1}.

bonding with OH of CHA. On the other hand, these vibrations are shifted to (3286, 3350 cm^{-1}) and (3331 and 3130 cm^{-1}), respectively, confirming the formation of CT-complexes.

4. The IR Spectra of the formed CT complexes showed ν (NH^+) bands at 2750 and 2997 cm^{-1} for AP and AMP donor complexes with CHA confirming the formation of hydrogen bonded proton transfer complexes between OH of CHA and the ring nitrogen.
5. The IR Spectrum of CHA–ADMT CT complex showed a broad band at 3136 cm^{-1} for ν (NH_3^+) confirming the migration of CHA proton to the amino group of ADMT through intermolecular hydrogen bonding.
6. The FTIR spectrum of AMTD–CHA complex (Fig. 6F) showed that this complex is a critical hydrogen bonded one (50% proton transfer O...H...N) [45]. It showed a number of anomalies such as the appearance of continuous absorption band extending from 4000 to 400 cm^{-1} [46] and the appearance of a strong Evan hall at 790 cm^{-1} resulting from the coupling between the ring skeletal and protonic vibrations [47]. Another feature in Fig. 6F is the appearance of new vibrational bands at 515, 538, 567, 590 cm^{-1}, respectively. These bands are presumably attributed to the formation of NHN hydrogen bonding beside OHN one in AMTD–CHA complex [48].
7. The FTIR Spectra of the CT-complexes between CHA and AMMP and ADMP are presented in Fig. 7. Fig. 7A showed the FTIR spectrum of CHA–AMMP complex where the symmetric and asymmetric stretching vibrations of the amino group ν^{as} (NH_2), ν^{s} (NH_2) are recorded at 3196 and 3347 cm^{-1} compared with 3205 and 3326 for AMMP donor. The ν *(C═O)* is recorded at 1667 cm^{-1} compared with 1662 cm^{-1} for CHA. The shift of the amino and carbonyl vibrations in the complex compared with those for the donor and acceptor confirmed the formation of CT-complex between CHA and AMMP. An important finding in Fig. 7A is the appearance of ν (NH^+) at 2670 cm^{-1} asserting the migration of CHA phenolic proton to the ring nitrogen through intermolecular hydrogen bonding. The CT-complex formation between CHA and AMMP is further confirmed by the appearance of ν (C-Cl) at 839 cm^{-1}.
8. The FTIR spectrum of CHA–ADMP CT-complex is shown in Fig. 7B where a broad band at 3157 and a shoulder at 3200 cm^{-1} attributing to the asymmetric and symmetric stretching vibrations of the amino group are recorded. The disturbance of the amino group reflects the sensitivity of this group towards hydrogen bonding interaction. The recorded band at 2889 cm^{-1} is presumably attributed to ν (NH^+) and confirming the migration of CHA phenolic proton to the ring nitrogen through intermolecular hydrogen bonding. The ν *(C═O)* was recorded at 1657 cm^{-1} compared with 1667 and 1662 cm^{-1} for CHA–AMMP and CHA, respectively. The situation confirms the formation of bifurcated hydrogen bonding in this complex. The formation of such bond reduces the π electron density of ADMP and led to a lower value of K_{CT} as discussed previously. The formed CT-complex between CHA and ADMP is further confirmed by the appearance of ν *(C—Cl)* at 784 and 676 cm^{-1}, respectively.

3.9.3. ^{1}HNMR spectra

The proton transfer process from CHA to the donors was further confirmed by measuring the ^{1}HNMR spectra of the reactants and the formed complexes in DMSO-d_6. It has been found that, the phenolic proton of CHA is assigned at 9.15 ppm. The ^{1}HNMR signal of CHA disappeared in the complexes of AP, AMP, ADMT, ADMP and AMMP with CHA. Instead a new peaks are observed at 5.89, 5.78, 6.7 and 6.3 ppm for the complexes of AP, AMP, ADMP and AMMP, respectively, attributing to NH^+ proton. This situation confirmed the transfer of the phenolic proton of CHA to the ring nitrogen of these donors in concordance with the FTIR results. Concerning the complex CHA–ADMT, a signal at 4.62 ppm is recorded attributing to three protons NH_3^+ and confirming the proton transfer from CHA to the amino group nitrogen. The ^{1}HNMR spectra of the CT-complexes between the donors DMP, AMT and CHA included the peaks of the phenolic proton of CHA at 8.98 and 9.12 ppm, respectively. These results confirmed the absence of proton transfer in these complexes.

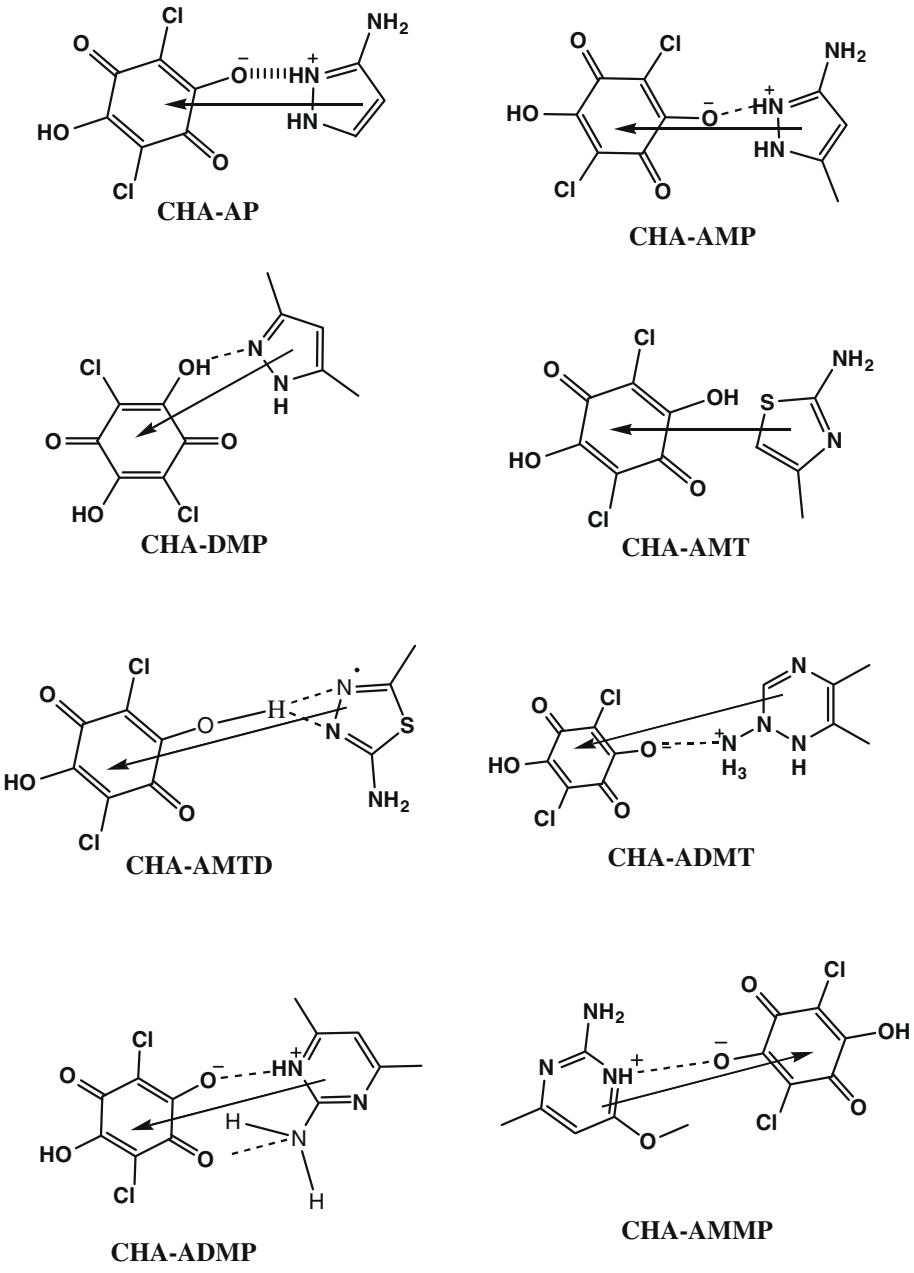

Scheme 4. Structures of the formed CT-complexes of CHA with donors.

Generally, one concludes that the molecular complexes between CHA and the donors are formed through electron and proton transfer except for DMP and AMT complexes. The suggested structures of the formed complexes are gathered in Scheme 4.

References

[1] S. Sadeghi, E. Karimi, Chem. Pharm. Bull. 54 (2006) 1107.
[2] I.A. Darwish, Anal. Chim. Acta 549 (2005) 212.
[3] H. Kusama, H. Sugihara, J. Photochem. Photobiol. A Chem. 181 (2006) 268.
[4] S.M. Andrade, S.M.B. Costa, R. Pansu, J. Collidal. Interf. Sci. 226 (2000) 260.
[5] K. Bradley, M. Briman, A. Satr, G. Gruner, Nano Lett. 4 (2004) 253.
[6] E.M. Koswer, Porg. Phys. Org. Chem. 3 (1965) 81.
[7] F.P. Fla, J. Palour, R. Valero, C.D. Hall, JCS Perkin Trans. 2 (1991) (1925).
[8] T. Roy, K. Dutta, M.K. Nayek, A.K. Mukherjee, M. Baneriee, B.K. Seal, JCS Perkin Trans. 2 (2000) 531.
[9] F. Yakuphanoglu, M. Arslan, Opt. Mater. 27 (2004) 29.
[10] F. Yakuphanoglu, M. Arslan, Solid State Comm. 132 (2004) 229.
[11] F. Yakuphanoglu, M. Arslan, M. Kucukislamoglu, M. Zengin, Sol. Energy 79 (2005) 96.
[12] B. Chakraborty, A.S. Mukherjee, B.K. Seal, Spectrochim. Acta A 57 (2001) 223.
[13] D.J. Brown, S.F. Mason, The Pyrimidines, Interscience Publishers, John Wiley and Sons, New York, 1962.
[14] C.B. Brouillette, C.T. Chang, M.P. Mertes, J. Med. Chem. 22 (1979) 1541.
[15] E. De Dlercq, J. Descamps, G. Huang, P. Torrence, Mol. Pharmacol. 14 (1978) 422.
[16] P.V. Danenberg, Biochim. Biophys. Acta 497 (1977) 73.
[17] A.D. Da Silva, A.S. Machado, C. Tempete, M. Rebort-Gero, Eur. J. Med. Chem. Chim. Ther. 29 (1994) 1149.
[18] S.M. Sondhi, M. Johar, S. Rajvanshi, S.G. Dastidar, R. Shukla, R. Raghubir, J.W. Lown, Aust. J. Chem. 54 (2001) 169.
[19] M. Kidwi, S. Saxena, S. Rastogi, R. Venkataraman, Curr. Med.Chem. Ant. Infect. 2 (2004) 269.
[20] S.K. Das, G. Krishnamoorthy, S.K. Dofra, Can. J. Chem. 78 (2000) 191.
[21] G.J. Ones, J.A. Jimenez, Tetrahydon Lett. 40 (1999) 8551.
[22] G. Smilh, R.C. Bott, A.D. Rae, A.C. Willis, Aust. J. Chem. 53 (2000) 531.
[23] G. Smilh, D.E. Lynch, K.A. Byriel, C.H. Kennard, J. Chem. Crystallogr. 27 (1997) 307.
[24] G. Smilh, D.E. Lynch, R.C. Bott, Aust. J. Chem. 51 (1998) 159.
[25] D.A. Skoog, Principle of Instrumental Analysis, third ed., Saunders College Publishing, New York, 1985 (Chapter 7).

[26] Adrien Albert, E.P. Serjeant, Ionization Constants of Acids and Bases, Methuen and Co Ltd., London, John Wiley and Sons Inc., New York, 1962 (Chapter 2).
[27] E.D. Berman, R. Thomas, P. Stahi, R. Scott, Can. J. Chem. 65 (1987) 1954.
[28] P. Job, Ann. Chim. Phys. 9 (1928) 113.
[29] R.S. Mulliken, J. Am. Chem. Soc. 74 (1952) 811.
[30] G.J. Haderski, Z. Chen, R.B. Krafccik, J. Mansovi, R.J. Baker, R.L. Towns, J. Phys. Chem. B 104 (2000) 2242.
[31] T. Kitamura, A. Hikita, H. Ishikawa, A. Fujimoto, Spectrochim. Acta A 62 (2005) 1157.
[32] A.B.P. Leve, Inorganic Electronic Spectroscopy, second ed., Elsevier, Amsterdam, 1985. p. 161.
[33] E.M. Voigt, C. Reid, J. Am. Chem. Soc. 86 (1964) 3930.
[34] R. Rathone, S.V. Linderman, J.K. Kochi, J. Am. Chem. Soc. 119 (1997) 9393.
[35] W.B. Person, J. Am. Chem. Soc. 84 (1962) 536.
[36] H.M. McConnel, J.J. Ham, J.R. Platt, J. Chem. Phys. 21 (1964) 66.
[37] a G. Briegleb, Z. Angew. Chem. 72 (1960) 401;
b G. Briegleb, Z. Angew. Chem. 76 (1964) 326.
[38] R.C. Weast, Hand Book of Chemistry and Physics, fifteenth ed., CRC Press, 1969–1970.
[39] A.F. Mosten, J. Chem. Phys. 24 (1956) 602.
[40] R.S. Becker, F.W. Worth, J. Am. Chem. Soc. 84 (1962) 4263.
[41] M. Pandeeswaran, K.P. Elango, Spectrochim. Acta A 65 (2006) 1148.
[42] J.C. Miller, J.N. Miller, Statistics for Analytical Chemistry, second ed., Ellis Horwood Limited, 1988.
[43] S. Akyuz, T. Akyuz, J. Mol. Struct. 551 (2003) 205.
[44] M. El-Sayed, S. Agrawl, Talanta 29 (1982) 535.
[45] M.M. Habeeb, Pol. J. Chem. 69 (1995) 1428.
[46] J. Kalenik, I. Majerz, L. Sobczyk, E. Grech, M.M. Habeeb, J. Chem. Soc. Faraday Trans. I 85 (1989) 3187.
[47] E. Grech, J. Kalenik, Z. Malarski, J. Chem. Soc. Faraday Trans. 79 (1983) 2005.
[48] M.M. Habeeb, Appl. Spectrosc. Rev. 32 (1997) 103.